

# A Mechanism for Photoinduced Effects In Tetracyanoethylene-Based Organic Magnets

Serkan Erdin and Michel van Veenendaal

Department of Physics, Northern Illinois University, DeKalb, IL, 60115  
& Advanced Photon Source, Argonne National Laboratory,  
9700 South Cass Avenue, Argonne, IL, 60439

The photoinduced magnetism in manganese-tetracyanoethylene (Mn-TCNE) molecule-based magnets is ascribed to charge-transfer excitations from manganese to TCNE. Charge-transfer energies are calculated using Density Functional Theory; photoinduced magnetization is described using a model Hamiltonian based on a double-exchange mechanism. Photoexciting electrons from the manganese core spin into the lowest unoccupied orbital of TCNE with photon energies around 3 eV increases the magnetization through a reduction of the canting angle of the manganese core spins for an average electron density on TCNE less than one. When photoexciting with a smaller energy, divalent TCNE molecules are formed. The delocalization of the excited electron causes a local spin flip of a manganese core spin.

PACS numbers: 75.50.Xx, 75.90.+w, 78.90.+t

In recent years, optical control of magnetic properties has drawn a great deal of attention [1]. Photoinduced changes in magnetic order were extensively studied in a variety of systems, including spin-crossover complexes [2], magnetic heterostructures [3], and manganese films [4]. Photoinduced effects were recently reported in molecule-based compounds, such as Co-Fe Prussian blue analogs [5, 6] and manganese-tetracyanoethylene,  $\text{Mn}(\text{TCNE})_x \cdot y(\text{CH}_2\text{Cl}_2)$  ( $x \approx 2$ ,  $y \sim 0.8$ ) [7]. In these compounds, magnetization induced by illumination with visible light can be partially eliminated by using light with a longer wavelength. In the Prussian blue analogs, the increase in magnetization is attributed to a low-spin to high-spin transition that is triggered by photoinduced charge transfer [8]. In the case of  $\text{Mn}(\text{TCNE})_x \cdot y(\text{CH}_2\text{Cl}_2)$ , which is the focus of this Letter, optical spectroscopy [7] suggests that the photoinduced magnetization can be related to a  $\pi \rightarrow \pi^*$  optical transition in TCNE, whereas a charge transfer between metal and ligand causes a decrease in magnetization. Despite the enormous technological potential of these organic-based molecular magnets with reversible photoinduced magnetization, little theoretical work has been done to describe the exact photoinduced states and the mechanism triggering photoinduced changes.

$\text{Mn}(\text{TCNE})_x \cdot y(\text{CH}_2\text{Cl}_2)$  is an electron transfer salt in which both Mn ion and the organic molecule TCNE carry spins;  $\text{CH}_2\text{Cl}_2$  is a solvent. According to Mössbauer spectroscopy studies, the transition-metal ion is divalent with manganese in a high-spin state [9]. The cyanocarbon acceptor  $\text{TCNE}^-$  has an unpaired electron in the  $\pi^*$  molecular orbital. The Mn ion and TCNE molecule are coupled antiferromagnetically with a critical temperature of 75 K [10]. At 2.5 K, the magnet exhibits a transition to a spin glass-like state [10]. Although the exact structure of the compound is unknown to date, experimental evidence suggests that Mn-TCNE forms a three-dimensional network in which each Mn ion is surrounded by up to six

TCNE molecules [11]. The lack of sufficient information on the structure limits the use of *ab initio* quantum chemistry calculations on this magnet.

Experimentally, it has been observed that the magnetization of the compound increases upon argon laser excitation in the region  $\sim 2.54 - 3.00$  eV and reaches saturation in 6 h, while the excitation in the region  $\sim 1.8 - 2.5$  eV results in partial reduction of the photoinduced magnetization. The photoinduced effects persist for several days at low temperature. Heating the molecular magnet up to 200 K after illumination of light does not fully erase the photoexcited state although photoinduced effects are not observed above 75 K. This implies that magnetic exchange alone does not explain the metastable state. In this Letter, we show that the excitation energies for photoinduced magnetization and demagnetization correspond to electronic transitions between Mn and TCNE with different valencies. Using Monte-Carlo simulations for a model Hamiltonian, we demonstrate that the magnetic interactions between the manganese spins depend dramatically on the valency of the TCNE molecule, explaining the changes in magnetization resulting from the photoinduced charge transfers.

First, we need to understand the nature of the transitions made for different excitation energies. To this end, we performed unrestricted density functional calculations using GAUSSIAN 03 software [12] with local spin density approximation [13]. The polarizable-conductor calculation model was used [14], to take into account the effects of the solvent. For the TCNE molecule, Dunning's correlation-consistent double- $\zeta$  basis set was taken, and an effective core potential (LANL2) was used for the core electrons of the Mn atom. Calculations for a Mn and TCNE cluster show that the excitation energies used experimentally correspond to excitations from the Mn  $e_g$  states to the TCNE molecule. In the ground state, manganese has a  $t_{2g}^3 e_g^2$  configuration with a spin  $S = 5/2$  and is octahedrally coordinated by TCNE molecules. Af-

ter photoexcitation, the Mn ion will be in a trivalent  $t_{2g}^3 e_g$  state with  $S' = 2$ , see Fig. 1(a). The energy for the excitation  $\text{Mn}^{2+} \text{TCNE}^- \rightarrow \text{Mn}^{3+} \text{TCNE}^-$  is 3.18 eV. The presence of neutral organic molecules in a strongly disordered compound such as Mn-TCNE is likely since some TCNEs can be disoriented and uncoupled to the Mn ions due to the solvent. The calculation slightly overestimates the transition energies due to a lack of band effects because of the finite size of the cluster and simplifications in the description of the polarizability of the solvent. The photoexcited state is expected to be mostly stable since the  $\text{Mn}^{3+}$  ion is Jahn-Teller active and the charge transfer induces a distortion of the TCNEs surrounding the Mn ion. Experimentally, it has been seen that the photoinduced magnetization is accompanied by lattice distortions [15]. Because the polaronic state does not depend on the magnetic order, it also explains why the photoinduced excited state is not fully erased when the temperature is raised above the critical temperature. Relaxation is further complicated by the fact that the  $e_g$  states couple only weakly to the TCNE valence states, which primarily consist of  $\pi$ -bonding orbitals. Photoinduced demagnetization is ascribed to the transition  $\text{Mn}^{2+} \text{TCNE}^- \rightarrow \text{Mn}^{3+} \text{TCNE}^{2-}$ , see Fig. 1(b), which occurs at 2.87 eV. The energy for this transition is lower due to the electrostatic interaction between the Mn and the TCNE. Therefore, when tuning the magnetization by illumination with visible light, effectively one changes the number of valence electrons by transferring electrons from the Mn core spin to the lowest unoccupied orbital on TCNE. By varying the wavelength of the light, one can create different oxidation states of the TCNE that, due to their different coupling to the manganese core spins, allows a decrease and increase in magnetization.

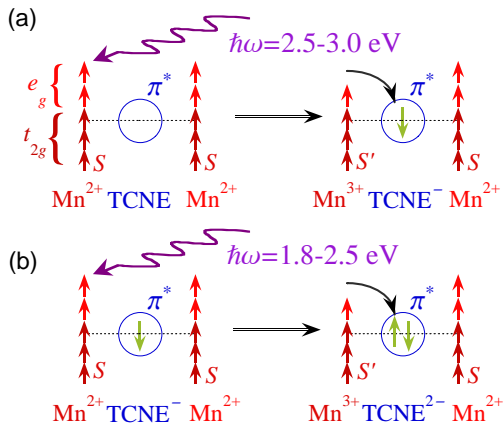


FIG. 1: (a) The charge-transfer process made for a photon energy of  $\hbar\omega = 2.5-3.0$  eV. An  $e_g$  electron from the Mn  $S = 5/2$ , which consists of 3  $t_{2g}$  electrons and 2  $e_g$  electrons, is transferred to the  $\pi^*$  orbital, the lowest unoccupied state of the TCNE molecule, leaving a core spin with  $S' = 2$ . (b) For lower incident photon energies, electrons are transferred to a  $\text{TCNE}^-$  molecule giving rise to a doubly occupied  $\pi^*$  orbital.

In order to describe how the photoinduced charge transfers between manganese and TCNE can have a strongly different impact on the magnetization, we use a model that captures the magnetic couplings between the manganese core spins and perform Monte-Carlo calculations to determine the magnetic properties. Of the TCNE, we retain the  $\pi^*$  orbital, which is the lowest unoccupied molecular orbital. We treat the manganese core spins classically. This approach is similar to the double-exchange mechanism [16, 17, 18] often used in the colossal magnetoresistive manganites. The Hamiltonian is given by

$$H_0 = -t \sum_{ij\sigma} \sin \frac{\theta_{j\sigma} - \theta_i}{2} (d_i^\dagger c_{j\sigma} + c_{j\sigma}^\dagger d_i) + \sum_i \varepsilon_d d_i^\dagger d_i + \sum_j \varepsilon_{\pi^*} c_{j\sigma}^\dagger c_{j\sigma} + J_{AF} \sum_{ii'} \mathbf{S}_i \cdot \mathbf{S}_{i'},$$

where  $c_{i\sigma}^\dagger$  creates an electron with spin  $\sigma$  on a  $\pi^*$  orbital of TCNE and  $d_j^\dagger$  creates an electron on the effective  $d$  orbital of the Mn site. The latter operator is not assigned a spin, since the spin of the conduction electrons is always antiparallel to that of the manganese core spin. Manganese and TCNE sites are labelled by  $i$  and  $j$ , respectively. The hopping amplitude between manganese and the  $\pi^*$  orbital is  $t$ .  $\theta_{i\sigma}$  is the angle of an electron on  $i$ 'th ligand, which is 0 or  $\pi$  for  $\sigma = \uparrow$  and  $\downarrow$ , respectively;  $\theta_j$  is the angle of classical manganese core spin at  $j$ 'th site.  $\varepsilon_d$  and  $\varepsilon_{\pi^*}$  are the energies for  $d$  and  $\pi^*$  orbitals, respectively. The last term in  $H_0$  is a superexchange interaction between two core spins mediated through the highest occupied molecular orbital of TCNE. We also include the Coulomb interaction on the TCNE molecule,

$$H_U = \sum_j U n_{j\uparrow} n_{j\downarrow}, \quad (1)$$

where  $U$  is the strength of the Coulomb interaction between two electrons in a  $\pi^*$  orbital. In our calculations, we first construct the Hamiltonian matrix for  $H_0$  for a given core spin configuration in a lattice. Since the structure is as yet unknown, we carry out our calculations on a two-dimensional lattice. In doing so, we both preserve the stoichiometry and use the two-dimensional symmetry of TCNE molecule. A unit cell contains one metal site at site  $(0, 0)$  and two ligands at sites  $(a/2, 0)$  and  $(0, a/2)$ , where  $a$  is the distance between two manganese atoms. For our calculations, we choose a lattice of  $4 \times 4$  unit cells and impose periodic boundary conditions, giving a matrix size of  $5N^2$ . In our model, we take  $t = 0.2$  eV,  $\varepsilon_d - \varepsilon_{\pi^*} = 1.5$  eV,  $U = 1$  eV. The value of  $J_{AF} S^2$  varies between 0.01 – 0.1 eV. For each Monte-Carlo step, we calculate eigenvalues and eigenvectors of the Hamiltonian with direct diagonalization. The Coulomb repulsion on the TCNE molecule is calculated within the Hartree-

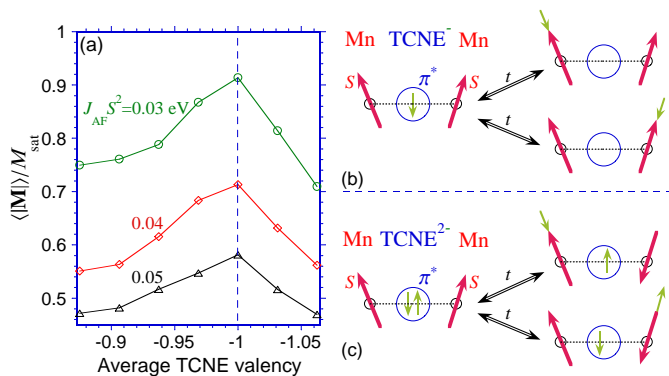


FIG. 2: (color online) (a) The normalized magnetization  $\langle |\mathbf{M}| \rangle / M_{\text{sat}}$ , where  $M_{\text{sat}}$  is the saturation magnetization, as a function of the average TCNE valency for superexchange coupling strengths  $J_{\text{AF}} S^2 = 0.03, 0.04$ , and  $0.05$  eV. (b) Schematic showing how the delocalization of an unpaired electron stabilizes the ferromagnetic exchange. The left side shows the lowest configuration; the right side shows the hopping processes that stabilize the magnetic coupling. (c) Schematic showing how the delocalization of two  $\pi^*$  electrons stabilizes the antiferromagnetic exchange.

Fock limit,

$$\langle U \rangle = \sum_j \langle \Psi_0 | U n_{j\uparrow} n_{j\downarrow} | \Psi_0 \rangle, \quad (2)$$

where  $|\Psi_0\rangle$  is the lowest many-body state of  $H_0$  obtained by filling the eigenstates up to the chemical potential using the Fermi-Dirac function for a finite temperature. In our Monte-Carlo calculations, for a given number of valence electrons, we calculate the average magnetization  $\langle |\mathbf{M}| \rangle$  of the whole lattice and average angles of core spins,  $\langle \theta_i \rangle$ , at different values of  $J_{\text{AF}}$ . For average magnetization calculations, we only consider the contribution of the manganese core spins. In our calculations, we take 8000-32000 Monte-Carlo steps in total, sufficiently larger than the 1000-5000 Monte-Carlo steps needed to establish the equilibrium state. We choose a low temperature of 5 K to minimize the temperature fluctuations.

The central result is shown in Fig. 2(a), where we see a significant change in the magnetization when electrons are transferred from manganese to TCNE for different values of the superexchange coupling. If not all the TCNE are ionized in the initial state, illumination with light creates a charge-transfer excitation from the Mn core spin to the valence band consisting of the TCNE  $\pi^*$  states and the Mn  $3d$  states antiparallel to the core spin. The magnetization increases up to a formal valency of  $-1$  for TCNE. The number of electrons in the valence band can be further increased by exciting with light having a smaller energy creating divalent TCNE molecules. However, these excitations lead to a decrease in magnetization, see Fig. 2(a).

To understand the trends in magnetization, we have to

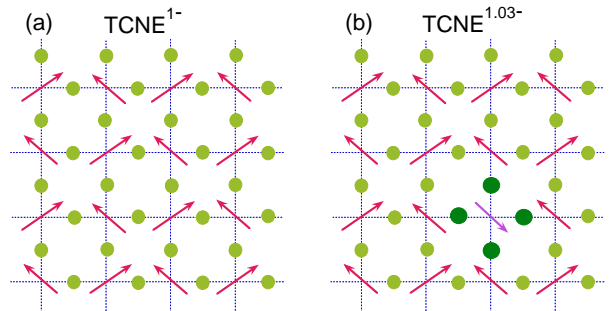


FIG. 3: (color online) (a) Canted spin state for an average TCNE valency of  $-1$  (the actual electron density on TCNE is  $0.97$ ). The arrows indicate the manganese core spins. The circles indicate the TCNE positions. (b) Spin state for an average TCNE valency of  $-1.03$ . Note that the excited electron is delocalized over the TCNE molecules surrounding the flipped spin, where the average density is  $1.2$  electrons (indicated by the larger dark-green circles).

distinguish the regions where the average TCNE valency is less and greater than  $-1$ . Figure 2(b) shows schematically how two manganese core spins are coupled ferromagnetically by an unpaired  $\pi^*$  electron. For parallel core spins, the conduction electron can lower its kinetic energy by coupling to the empty Mn  $t_{2g}$  states. To obtain a ferromagnetic ground state, it is important to include the Coulomb interaction on the TCNE ions. This can be understood as follows. In the ferromagnetic state, the coupling to the manganese core spins splits the TCNE states in a spin-up and spin-down band. For an average TCNE valency of  $-1$ , the spin-down band (antiparallel to the core spins) is full, and there is no kinetic energy gain. However, for an antiferromagnetic configuration of manganese spins, kinetic energy can still be gained since the TCNE  $\pi^*$  orbital can be doubly occupied. Therefore, this state is lower in energy when the average electron density per TCNE is greater than  $\frac{1}{2}$ , even in the absence of a superexchange interaction between the core spins. However, the antiferromagnetic state becomes unfavorable in the presence of a Coulomb interaction on the TCNE.

The behavior as a function of TCNE valency is a result of the competition between the ferromagnetic coupling mediated by the unpaired TCNE  $\pi^*$  electrons and the antiferromagnetic superexchange through the occupied TCNE  $\pi$  orbitals. Our Monte-Carlo simulations show that a canted spin state is formed. A typical example is shown in Fig. 3(a) for  $J_{\text{AF}} S^2 = 0.05$  eV. To study the average canting angle of the Mn core spins with respect to the magnetization axis, we define  $\langle |\theta| \rangle = \frac{1}{N^2} \sum_i \langle |\theta_i| \rangle$ . Figure 4(a) shows  $\langle |\theta| \rangle$  as a function of the strength of the superexchange  $J_{\text{AF}} S^2$ . We see that canting occurs for a critical superexchange coupling, here  $J_{\text{AF}} S^2 = 0.02$  eV, see Fig. 4(a). Of interest for the photoinduced effect is the change in canting angle as a function of the average TCNE valency. From Fig. 4(b), we see that a change in TCNE valency of  $0.1$  electrons can cause a change in the

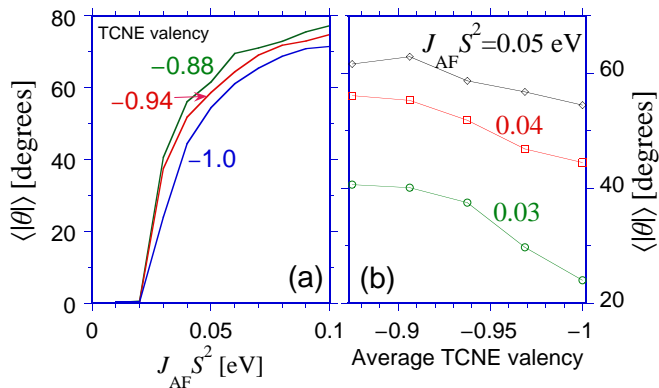


FIG. 4: (a) The average canting  $\langle|\theta|\rangle$  with respect to the magnetization axis as a function of the strength of the superexchange coupling  $J_{AF}S^2$ . (b) The average canting  $\langle|\theta|\rangle$  as a function of the average TCNE valency for  $J_{AF}S^2 = 0.03, 0.04, \text{ and } 0.05$  eV.

average canting angle of about  $10\text{-}20^\circ$ . An increase in the number of unpaired electrons on TCNE leads to a stronger ferromagnetic coupling and hence a decrease of the canting angle. Therefore, photoinduced transitions for electron densities less than one electron per TCNE, increase the magnetization, see Fig. 2(a).

The situation drastically changes when charge-transfer excitations are made with a smaller energy, where optical transitions are made from the manganese core spin to the TCNE, creating a doubly occupied  $\pi^*$  orbital. This changes the coupling between the manganese spins from ferromagnetic to antiferromagnetic, as is shown schematically in Fig. 2(c). Instead of letting one  $\pi^*$  electron hybridize with both neighboring manganese atoms, it is kinetically more advantageous to flip one of the manganese spins allowing both  $\pi^*$  electrons to hybridize. For a larger system, the excited electron delocalizes over the TCNE molecules surrounding the flipped spin, see Fig. 3(b). Note that the average valency of the TCNE surrounding the flipped spin is not  $-2$ , but closer to  $-1.2$ , explaining why divalent TCNE molecules are not observed experimentally in, e.g., Mössbauer spectroscopy [9].

Summarizing, we have described a mechanism for photoinduced magnetism in Mn-TCNE systems. Illumination with visible light causes charge-transfer transitions from the Mn core spins to the valence shell consisting of the Mn  $3d$  states antiparallel to the core spins and the TCNE  $\pi^*$  orbitals. When the average density of electrons per TCNE is less than one, photoexciting electrons into the valence states strengthens the double-exchange coupling between the Mn core spins. This decreases the canting angle and increases the magnetization. Illumination with a larger wavelength creates divalent TCNE

molecules. The magnetic coupling dramatically changes and locally core spins are flipped, causing a decrease in magnetization. The  $S' = 2$  core spin created by the photoexcitation is sensitive to Jahn-Teller distortions and forms a local polaron. Polaron formation can strongly influence the dynamics of the system and can provide a mechanism to explain the long lifetime of the photoinduced magnetic state.

The authors acknowledge Ken Ahn, A. J. Epstein, and J. S. Miller for fruitful discussions. This work was supported by the U.S. Department of Energy (DE-FG02-03ER46097), Research Cooperation and NIU's Institute for Nanoscience, Engineering, and Technology under a grant from the U.S. Department of Education. Work at Argonne National Laboratory was supported by the U.S. Department of Energy, Office of Basic Energy Sciences, under contract W-31-109-ENG-38.

- 
- [1] I. Zutic, J. Fabian, and S. Das Sarma, *Rev. Mod. Phys.* **76**, 323 (2004).
  - [2] Y. Ogawa, S. Koshihara, K. Koshino, T. Ogawa, C. Urano, and H. Takagi, *Phys. Rev. Lett.* **84**, 3181 (2000).
  - [3] S. Koshihara *et al.*, *Phys. Rev. Lett.* **78**, 4617 (1997).
  - [4] K. Matsuda, A. Machida, Y. Moritomo, and A. Nakamura, *Phys. Rev. B* **58**, 4203 (1997).
  - [5] O. Sato, T. Iyoda, A. Fujishima, and K. Hashimoto, *Science* **272**, 704 (1996).
  - [6] D. A. Pejakovic, J. L. Manson, J. S. Miller, and A. J. Epstein, *Phys. Rev. Lett.* **85**, 1994 (2000).
  - [7] D. A. Pejakovic, C. Kitamura, J. S. Miller and A. J. Epstein, *Phys. Rev. Lett.* **88**, 057202 (2002).
  - [8] T. Kawamoto, Y. Asai, and S. Abe, *Phys. Rev. Lett.* **86**, 348 (2001).
  - [9] J. Zhang, J. Ensling, V. Ksenofontov, P. Gutlich, A. J. Epstein and J. S. Miller, *Angew. Chem. Int. Ed. Engl.* **37**, 657 (1998).
  - [10] C. M. Wynn, M. A. Girtu, J. Zhang, J. S. Miller, and A. J. Epstein, *Phys. Rev. B* **58**, 8508 (1998).
  - [11] J. S. Miller and A. J. Epstein, *Chem. Commun.* **1998**, 1319.
  - [12] Gaussian 03, Revision C.02, M. J. Frisch, *et al.* Gaussian, Inc., Wallingford CT, 2004.
  - [13] J. C. Slater, *Quantum Theory of Molecular and Solids. Vol. 4: The Self-Consistent Field for Molecular and Solids* (McGraw-Hill, New York, 1974); S. H. Vosko, L. Wilk, and M. Nusair, *Can. J. Phys.* **58**, 1200 (1980).
  - [14] V. Barone and M. Cossi, *J. Phys. Chem. A* **102**, 1995, (1998).
  - [15] D. A. Pejakovic, C. Kitamura, J. S. Miller, and A. J. Epstein, *J. Appl. Phys.* **91**, 7176 (2002).
  - [16] C. Zener, *Phys. Rev.* **82**, 403 (1951).
  - [17] P. W. Anderson and H. Hasegawa, *Phys. Rev.* **100**, 675 (1955).
  - [18] P.-G. de Gennes, *Phys. Rev.* **118**, 141 (1960).